

PAPER • OPEN ACCESS

Development of an *in situ* injectable hydrogel containing hyaluronic acid for neural regeneration

To cite this article: Linh T B Nguyen *et al* 2020 *Biomed. Mater.* **15** 055005

View the [article online](#) for updates and enhancements.

You may also like

- [Effect of high-pressure deuterium annealing with high- stack onto \$\text{In}_{0.52}\text{Ga}_{0.47}\text{As}\$ MOS capacitors on 300 mm Si substrate](#)
Seung Heon Shin, Dae-Hyun Kim and Tae-Woo Kim
- [In Situ Atomic Force Microscopy Imaging of a Heteropolyanion onto a HOPG Electrode during Its Cyclic Voltammetry](#)
M. Rivera, S. Holguin, A. Moreno et al.
- [12-Silicotungstic Acid Doped Phosphoric Acid Imbibed Polybenzimidazole for Enhanced Protonic Conductivity for High Temperature Fuel Cell Applications](#)
Vinh T. Nguyen, Jason T. Ziolo, Yuan Yang et al.

Biomedical Materials



PAPER

OPEN ACCESS

RECEIVED

8 November 2019

REVISED

24 February 2020

ACCEPTED FOR PUBLICATION

22 April 2020

PUBLISHED

16 July 2020

Original content from this work may be used under the terms of the [Creative Commons Attribution 4.0 licence](#).

Any further distribution of this work must maintain attribution to the author(s) and the title of the work, journal citation and DOI.



Development of an *in situ* injectable hydrogel containing hyaluronic acid for neural regeneration

Linh T B Nguyen^{1,2} , Chia-Chen Hsu¹, Hua Ye¹ and Zhanfeng Cui¹

¹ Institute of Biomedical Engineering, Department of Engineering Science, University of Oxford, Oxford OX3 7DQ, United Kingdom

² Division of Biomaterials and Tissue Engineering, UCL Eastman Dental Institute, London WC1X 8LD, United Kingdom

E-mail: hua.ye@eng.ox.ac.uk

Keywords: hyaluronic acid, dopamine, injectable hydrogel, neural regeneration

Supplementary material for this article is available [online](#)

Abstract

In this work, a novel enzymatically crosslinked injectable hydrogel comprising hyaluronic acid (HyA), dopamine (DA), and 3-(4-hydroxyphenyl) propionic acid (HPA) conjugates was successfully developed. To the best of our knowledge, it is the first time that HPA is conjugated to a HyA-based backbone. *In situ* hydrogelation of HyA-DA-HPA occurred in the presence of hydrogen peroxide (H_2O_2) as an oxidant and horseradish peroxidase (HRP) as a catalyst. Proton nuclear magnetic resonance and Fourier transform infrared spectroscopy were used to characterize the chemical reactions between HyA, DA, and HPA. Gel formation completed between 3 s to 5 min depending on the concentrations of polymer, HRP, and H_2O_2 . Crosslinked HyA-DA-HPA gels acquired storage moduli ranging from ~ 100 Pa to $\sim 20\,000$ Pa (at $f = 2000$ rad s^{-1}). Biocompatibility of the hydrogels was examined with human mesenchymal stem cells (hMSCs) and human induced pluripotent stem cell-derived neural stem cells. The hydrogels made of 2.0 w/v% HyA-DA-HPA hydrogels, 0.24 U ml^{-1} HRP and ≤ 0.5 $\mu\text{mol ml}^{-1}$ H_2O_2 were found biocompatible with hMSCs cultured on and encapsulated within the hydrogels. Since HyA serves as a backbone of the extracellular matrix in the central nervous system (CNS) and DA acquires the ability to restore dopaminergic neurons, use of this injectable HyA-DA-HPA hydrogel for stem cell transplantation is a potential treatment strategy for CNS repair and regeneration.

1. Introduction

Hydrogels are one of the most promising polymeric biomaterials in tissue engineering for delivering cells, growth factors, peptides and drugs that aid tissue regeneration [1–4]. They facilitate efficient encapsulation and delivery of cells and/or soluble factors as they can be tailored to provide high oxygen permeability, supply nutrients and efficiently channel water-soluble metabolites through their hydrated matrix [4, 5]. One of the greatest challenges for its application in neural tissue engineering is the effective entrapment and delivery of cells and growth factors to the target site. The soft nature of the tissue, its extremely limited regenerative capability, as well as the lack of nutrient and oxygen perfusion in the wound sites could hinder the delivery and growth of cells [6]. In this regard, *in situ* injectable hydrogels, which can be injected as a liquid and solidify *in situ* to form a

substrate with ideal mechanical properties and the capability to support stem cell transplants, have been explored for neural repair [7]. Injectable hydrogels also allow a minimally invasive procedure, which may offer further benefits, including smaller incisions, reduced pain and scarring and short recovery times [8].

To date, a variety of natural and synthetic polymers, including alginate, collagen, and poly(lactic-co-glycolic acid) (PLGA), as well as decellularized extracellular matrix (ECM), have been utilized as supporting grafts to facilitate stem cell transplantation (reviewed in Chan *et al* 2017, Tuladhar *et al* 2018, and Nih *et al* 2016) [7, 9, 10]. For example, Ford *et al* achieved the generation of a functional and stable microvascular system by delivering co-cultures of neuronal progenitor cells and endothelial cells through a macro-porous polyethylene glycol (PEG)-based hydrogel system *in vivo* [11]. A hydrogel made

of self-assembling peptides has also been shown to support differentiation and maturation of human neural stem cells (NSCs) in 3D serum-free conditions *in vitro* and demonstrated its functional regenerative potential in rat spinal cord injuries [12].

Hyaluronic acid (HyA) is a linear polysaccharide serving as a major component in the central nervous system (CNS) ECM [13]. It binds to proteoglycans which further bind to tenascins, resulting in the structural backbone of the CNS [14]. Although HyA can be extracted from animal tissues, xeno-free HyA can be produced via bacterial fermentation [15]. In regard to its biocompatibility, its regulatory role in inflammation and glial scar formation, as well as the advantageous chemical tunability, HyA has become one of the most suitable materials for neural tissue engineering [16–18]. Previously, mechanically tunable HyA scaffolds for delivery of growth factors and cells have been shown to mediate and support survival and differentiation of neural cells both *in vitro* and *in vivo* [14, 19, 20]. To enhance cell-matrix interaction, adhesive molecules (i.e. collagen and RGD peptide) and heparin could be additionally functionalized into the HyA hydrogels to promote cell adhesion and sequestration of soluble factors [21].

Dopamine (DA) is one of the major neurotransmitters in the brain, playing a key role in brain aging and neurodegenerative diseases, particularly, Parkinson's disease [22]. In PC12 neuronal cells, it was reported that DA pre-treatment at a noncytotoxic concentration may serve as a potent inducer of cellular glutathione and NAD(P)H:quinone oxidoreductase 1, exerting neuroprotective effects [23]. Previously, the development of injectable hydrogel systems for local delivery of DA, DA-loaded microspheres, and DA-secreting cells has been reported [21, 24–27]. A hydrogel system made of chitosan, gelatin, and DA was shown to possess a sustained DA release profile without a burst release over the course of 500 h [25]. Implantation of a dextran dialdehyde crosslinked gelatin hydrogel loaded with DA could improve functional recovery in a 6-hydroxydopamine (6-OHDA)-rat hemiparkinsonian model, suggesting the potential application of DA-embedded hydrogel for treating Parkinson's disease [26]. Although there are a number of publications focusing on hydrogel systems for DA release, to the best of our knowledge, a hydrogel incorporating DA into its polymer backbone has never been reported.

In this study, we fabricated a novel hydrogel using HyA, 3-4-hydroxyphenylpropionic acid (HPA) and DA. While HyA is a strong hydrophilic anionic polysaccharide containing a large number of hydroxyl and carboxyl groups as hydrogen bond donors or acceptors, it can facilitate hydrogen bond formation and hydrogelation [28]. Previously, gelatin-based hydrogels formed by conjugating HPA into its backbone were found with higher adhesiveness compared to that of commercial fibrin glue [29].

It was suggested that a higher phenolic content in the polymer may result in higher cohesive and adhesive strength [29, 30]. In this study, we aim to design an injectable hydrogel system that is able to improve cellular incorporation and tissue attachment, as well as neuroprotective effects by incorporating both HPA and DA into our system, which has never been reported previously. We used an enzymatic chemical crosslinking process that includes horseradish peroxidase (HRP) and hydrogen peroxide (H_2O_2) to fabricate hydrogels of HyA, DA, and HPA. This crosslinking approach has been used to form fast gelling, non-toxic and stable hydrogels [31]. Our novel hydrogel was then tested for its biocompatibility. This hydrogel system based on HyA, the structural backbone of the CNS, and incorporating DA, which triggers some neuroprotective effects in the brain, can provide an alternative platform for delivering cells and growth factors to the CNS, particularly the brain, facilitating neural repair and regeneration.

2. Materials and methods

2.1. Materials

HyA ($M_w = 100$ KDa), DA hydrochloride, HPA, HRP type VI, 250–330 units mg^{-1} , H_2O_2 , N-hydroxysuccinimide (NHS), 1-ethyl-3-(3-dimethylaminopropyl)-carbodiimide hydrochloride (EDC-HCl), and 4-morpholineethanesulfonic acid (MES) are from Sigma-Aldrich (UK). Spectra/PorTM regenerated cellulose molecular weight cut-off (MWCO, 8000 Da) dialysis membrane is from Spectrum Chemical Mfg. Corp. (USA).

2.2. Synthesis of HyA-DA, HyA-DA-HPA polymer, and HyA-DA-HPA hydrogel

2.2.1. Synthesis of HyA-DA

HyA-DA was synthesized by carbodiimide coupling chemistry (figure 1). Briefly, HyA (1 g) was dissolved in MES buffer (100 ml, 0.5 M, pH 5.5) and EDC (1.152 g, 3.0 mmol) and NHS (0.692 g, 3.0 mmol) were added to the HyA solution. To prepare a series of HyA-DA conjugates with catechol groups in various ratios, HyA was reacted with different concentrations of DA: 0.191 g (0.5 mmol), 0.574 g (1.5 mmol), 1.148 g (3.0 mmol), and 1.914 g (5.0 mmol), respectively. The reaction mixtures were stirred at room temperature for 4 h while maintaining pH 5.5. The solution was purified by dialysis for 3 d against acidified deionized water (pH 5.5) to inhibit oxidation of catechol groups and 1 d against neutral water for pH adjustment. The dialysis solution was refreshed every day.

2.2.2. Synthesis of HyA-DA-HPA polymer

HPA (10 mmol) was mixed in distilled water:DMF (3:2). 13.9 mmol NHS with 1.91 M EDC solution was added and stirred for 5 h at room temperature, pH

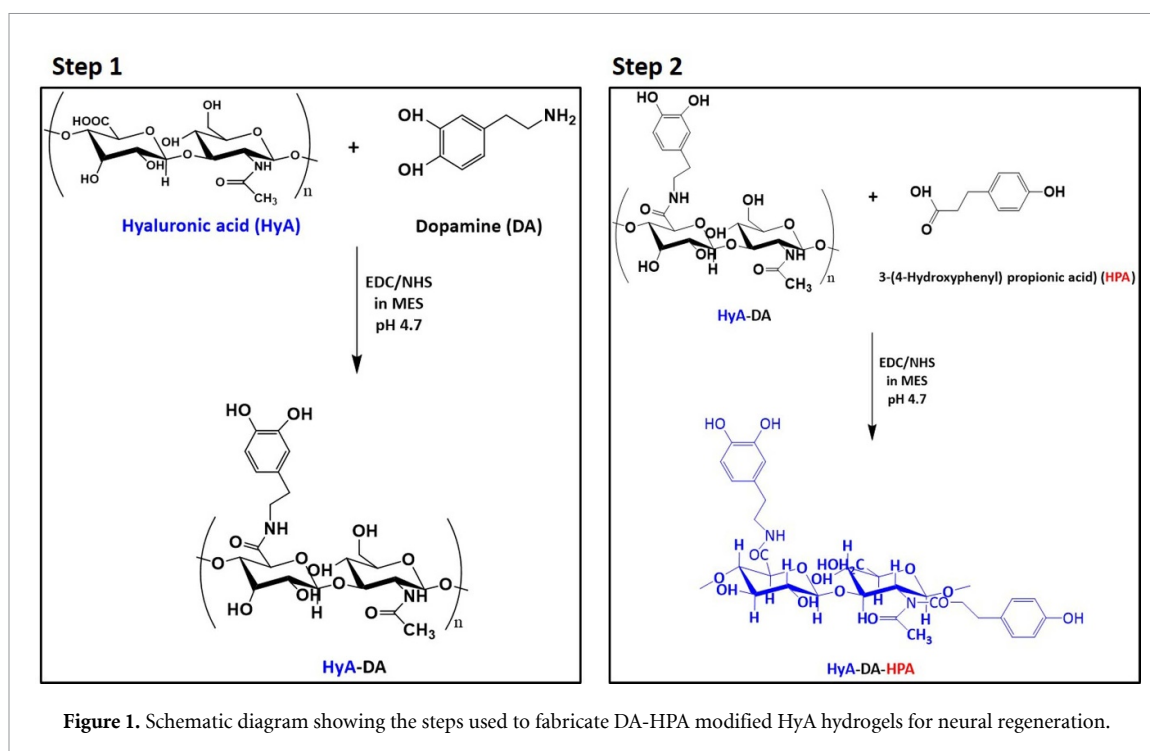


Figure 1. Schematic diagram showing the steps used to fabricate DA-HPA modified HyA hydrogels for neural regeneration.

4.7. The NHS, EDC solution was then added to the HyA-DA solution and stirred for 12 h at room temperature, pH 4.7. HyA-DA-HPA was dialyzed using the same process as HyA-DA and then freeze-dried for 2 d to obtain HyA-DA-HPA polymer.

2.2.3. Synthesis of HyA-DA-HPA gel

HyA-DA-HPA polymer, HRP, and H_2O_2 solutions in different concentrations were individually prepared by dissolution in phosphate buffered saline (PBS) at pH 7.4. Polymer concentrations of 0.5, 1.0, 1.5, 1.75 and 2.0 w/v%, HRP concentrations of 0.05, 0.08, 0.1, 1.12, 0.16 and 0.24 U ml^{-1} , and H_2O_2 concentrations of 0.15, 0.25, 0.5, 0.75 and 1.0 $\mu\text{mol ml}^{-1}$ were used. HyA-DA-HPA gels were obtained by peroxidase-catalyzed gelation at 37 °C.

2.3. Characterization of polymer

2.3.1. Fourier transform infrared (FTIR) spectrometers
FTIR can determine the structure of molecules by measuring the molecule's characteristic absorption of infrared radiation [32]. After finishing the dialysis step, the HyA-DA-HPA polymer solutions were freeze-dried to obtain the cotton-like solids and these materials were then used for FTIR analysis. The successful synthesis of HyA-HPA and HyA-HPA-DA was determined by analyzing the spectra obtained by FTIR spectra (Tensor 27, Bruker, USA) using the OPUS Data Collection Program. Highly sensitive liquid nitrogen cooled MCT (mercury-cadmium-telluride) detector was used.

2.3.2. Nuclear magnetic resonance (NMR)

The structure of HyA, DA, HPA, HyA-DA, and HyA-DA-HPA were determined using proton NMR (^1H NMR)-400 MHz (AVIIIHD 400 nanobay—aka AVH 400, Bruker, USA). Deuterium oxide (D_2O) was used as the solvent.

2.3.3. Scanning electron microscope (SEM)

Lyophilized samples were mounted on holders. The surface morphologies of the HyA-DA-HPA before and after gel formation were observed by SEM (Carl Zeiss Evo LS15 VP- SE, BSE, VPSE, EPSE detectors, Zeiss, Germany) at an accelerating voltage of 10 kV. Before the SEM investigation, the samples were coated with gold by SC7620 Mini Sputter (Quorum Technologies, UK).

2.3.4. Rheological measurement

Rheological measurements of the hydrogel formation were performed with a Diffusing Wave Spectroscopy system (LS instruments, CH). Hydrogel solutions with 200 nm diameter polystyrene tracer particles (10% w/v, Sigma-Aldrich) were used to determine how the gel network interaction modulates the tracer particles' thermal motion. The measurements were taken at 37 °C using 2 mm glass cuvettes in thickness (LS Instruments, CH). Solutions of HRP (0.24 U ml^{-1}) and H_2O_2 (0.25 $\mu\text{mol ml}^{-1}$) were added to an aqueous solution of HyA-DA-HPA (0.5%, 1.0%, 1.5%, 1.75% and 2% (w/v)), pre-warmed at 37 °C. The solution was vortexed and then immediately transferred into the cuvettes. The cuvettes were sealed with a lid and placed into the rheology system.

2.3.5. Gelation time

The HyA-DA-HPA hydrogels (400 μl) were prepared in 0.01 M PBS (pH 7.4) in 1 ml vials at room temperature. The polymer solution, the HRP, and H_2O_2 solution were pre-heated at 37 °C before mixing and loading into the double syringe. Briefly, the polymer solution (200 μl , 4.0 w/v%) was mixed with HRP solution (100 μl of 0.96 U ml^{-1} of stock solution) and H_2O_2 (100 μl of 4.0 $\mu\text{mol ml}^{-1}$ of stock solution) by gentle shaking. The time taken for gel formation (gelation time) was determined using a test tube inversion method [33–35]. The gelation time was recorded as the time when the gel mass stopped flowing after inversion. The gelation time was measured at different concentrations of HRP, H_2O_2 , and polymer.

2.4. Cell culture

2.4.1. Human GFP-MSC cells

Green fluorescence protein (GFP) was cloned into human mesenchymal stem cells (MSC, kindly provided from the Department of Pediatrics and Adolescent Medicine, LKS Faculty of Medicine, The University of Hong Kong). Briefly, primary mesenchymal cells obtained from unfractionated bone marrow mononuclear cells of a healthy donor were cultured for 2 months. Cells were infected with a VSV-G (expressing the G glycoprotein of the vesicular stomatitis virus) pseudotyped retroviral vector that contained the hTERT and GFP genes, separated by an internal ribosome entry site (IRES), under the control of the murine stem cell virus (MSCV) long-terminal repeat (LTR). The GFP⁺ and GFP⁻ MSCs were then separated with a fluorescence-activated cell sorter (MoFlo, Cytomation, Fort Collins, CO, USA) [36]. MSC-GFP were cultured in Dulbecco's modified Eagle's medium (DMEM 1.0 mg l^{-1} of glucose, Gibco BRL, Gaithersburg, MD, USA) supplemented with 10% (v/v) fetal bovine serum (FBS, Gibco BRL) and 0.1% (v/v) penicillin-streptomycin (PS, Gibco BRL).

2.4.2. Human iPSC-derived NSCs

The human induced pluripotent stem cell (iPSC) line, line 010S-1, generated at the Highfield Unit, Warneford Hospital, Oxford, was maintained on Matrigel (Corning, UK)-coated culture plates in feeder-free culture conditions with the use of chemically defined mTeSRTM1 media (STEMCELL Technologies, UK) and Essential 8 media (Thermo Fisher Scientific, UK). Colonies of human iPSCs were passaged by dissociation with 0.5 mM EDTA (pH 8.0; Thermo Fisher Scientific) in sterile phosphate buffer solution (PBS) when they reached 80–90% confluence. Neural differentiation was based on published protocols with some modifications [37, 38]. Briefly, human iPSC cultures were used for neural conversion when they reached confluence. Neural

Basal Medium were prepared for neural differentiation by mixing 1:1 ratio of [Advanced DMEM/F-12 medium (Thermo Fisher Scientific), 1 v/v% N-2 supplement (Invitrogen, UK), 0.2 v/v% B27 Supplement (Invitrogen), 1 v/v% penicillin/streptomycin (Invitrogen), 1 v/v% GlutaMAX (Invitrogen)] and [Neurobasal Medium (Thermo Fisher Scientific), 2 v/v% B27 Supplement (Invitrogen), 1 v/v% MEM Non-Essential Amino Acids (Thermo Fisher Scientific), 1 v/v% penicillin/streptomycin (Invitrogen), 1 v/v% GlutaMAX (Invitrogen)]. The cells were differentiated into neuroectoderm by dual SMAD signaling inhibition [39], using neural induction medium [Neural Basal Medium supplemented with SB431542 (10 μM ; Calbiochem, UK) and InSolutionTM AMPK Inhibitor, Compound C (2 μM ; Calbiochem, UK)] for 7–10 d. After enzymatic dissociation, we then passaged and plated down the NSCs on laminin (Sigma-Aldrich)-coated plates in the Neural Basal Medium. After 3–5 d culture, human iPSC-derived NSCs proliferated and formed neural rosette structures. The cell culture media was then changed into F20 Medium [Neural Basal Medium supplemented with 20 ng ml^{-1} FGF2 (PeproTech)]. NSCs were sub-cultured every 5–7 d on laminin-coated plates for the first few passages and on Matrigel-coated plates for later passages.

2.4.3. Immunostaining and fluorescence microscopy

For characterization of human iPSC-derived NSCs, cells were fixed in 3.7 v/v% paraformaldehyde (Sigma-Aldrich) for 15 min, permeabilized with 0.2 v/v% Triton X-100 (Sigma-Aldrich) for 10 min, and blocked with 3 v/v% goat serum (Sigma-Aldrich) for 30 min. Cells were then incubated for 1 h with primary antibodies, Nestin (1:500; Millipore, UK), PAX6 (1:200; Sigma-Aldrich), and β III-tubulin (1:1000; Sigma-Aldrich), followed with incubation of Alexa Fluor secondary antibodies (ThermoFisher Scientific) and NucBlue Live ReadyProbesTM Reagent (Invitrogen) or Hoechst 33342 staining solution (ThermoFisher Scientific) for 30 min. Each step above was followed by 3 washes with PBS. Cell images were acquired with a Nikon Eclipse Ti-E inverted fluorescence microscope (Nikon Instruments, Inc, UK).

2.5. Cellular responses towards HyA-DA-HPA hydrogels

2.5.1. Cell viability of MSCs on the surface of the HyA-DA-HPA gel

The effect of varying H_2O_2 concentration (0.15, 0.25, 0.5, 0.75 and 1.0 $\mu\text{mol ml}^{-1}$) on the viability of MSC was determined. The concentration of HRP and polymer was kept at 0.24 U ml^{-1} HRP and 2.0 w/v% polymer, respectively. Hydrogels were injected into 48-well plates and MSCs were then cultured on top of the prepared hydrogels and incubated for 1, 2 and 7 d. Cell viability was determined by CCK-8 assay (Sigma-Aldrich) with the absorption at 450 nm.

2.5.2. Cellular responses of MSCs towards

HyA-DA-HPA hydrogels

Hydrogels (400 μl) made with 2% (w/v) HyA-DA-HPA final concentration, 0.5 $\mu\text{mol ml}^{-1}$ H_2O_2 and 0.24 U ml^{-1} HRP (prepared in cell culture medium) were mixed with MSCs and injected into a 48-well culture plate and incubated for 1, 2 and 7 d. GFP expressing MSCs encapsulated within the hydrogels were imaged using a cooled CCD camera (EXI blue; QImaging, UK) attached to a Nikon Eclipse Ti-E inverted fluorescence microscope.

2.5.3. Cellular responses of human iPSC-derived NSCs towards HyA-DA-HPA hydrogels

Hydrogels (400 μl) made with 2% (w/v) HyA-DA-HPA final concentration, 0.5 $\mu\text{mol ml}^{-1}$ H_2O_2 and 0.24 U ml^{-1} HRP were injected into a 48-well culture plate. Human iPSC-derived NSCs were seeded on top of the prepared hydrogels and control substrates (tissue culture polystyrene (TCP) plates) with a cell density of 100 k cells cm^{-2} in Neural Basal Medium supplemented with 10 $\mu\text{g ml}^{-1}$ laminin and 10 ng ml^{-1} BDNF (PeproTech). Cell viability was evaluated using Calcein AM (Abcam), which stained viable cells with green fluorescence through the reaction of Calcein AM with intracellular esterase, and DRAQ5TM (Abcam), which is a cell permeable far-red fluorescent DNA dye staining cell nuclei. The viability was determined by the percentage of viable cells to total cell nuclei on day 1 and day 3.

2.6. Statistical analysis

The MSC experiments were conducted with 4 independent replicates and the human iPSC-derived NSC experiments were conducted with 3 independent experiments and 9 replicates in total. Statistical analysis of the MSC experiments was performed with one-way analysis of variance (ANOVA) with Tukey's honest significant difference post hoc test and the statistical analysis of the human iPSC-derived NSC experiments was performed with two-sample t-tests. A value of $p < 0.05$ was considered statistically significant.

3. Results and discussion

3.1. Formation of HyA-DA-HPA polymer

In the functionalized HyA hydrogels, HPA is used to aid both the attachment of incorporated cells as well as the attachment of the scaffold to the site so that the scaffold is less likely to become detached after transplantation [29, 30]. DA, on the other hand, has been used to treat Parkinson's disease patients or to reduce the death of dopaminergic neurons, such that this hydrogel may function to aid neural viability [22, 23]. To combine these three compounds together, the synthesis of HyA-DA-HPA was achieved via a two-step reaction (figure 1). Firstly, HyA-DA was conjugated

from HyA and DA through a general carbodiimide/active ester-mediated coupling reaction with different ratios of catechol groups. After purification of the HyA-DA conjugates by dialysis, instead of lyophilizing to obtain HyA-DA conjugates, HPA was introduced to the purified HyA-DA conjugate solution for synthesizing the HyA-DA-HPA conjugate. This reaction was carried out between amine groups of HyA and succinimide-activated HPA. Finally, a freeze-drying step was carried out to obtain the lyophilized HyA-DA-HPA polymer.

3.2. Characterization of HyA-DA-HPA polymer

Functional groups and chemical bonds of HyA-DA conjugates were identified by FTIR, shown as supplementary figure S1 (available online at stacks.iop.org/BMM/15/055005/mmedia). A broad-band centered at 3300 cm^{-1} was assigned to the vibration of the hydroxyl groups of HyA. The absorption of HyA-DA conjugates exhibited additional peaks consistent with the main vibration modes of DA, such as the C-H vibration at 2850 cm^{-1} and the C = C ring stretching at 1520 cm^{-1} . The absorption peaks located at 1720, 1630 and 1410 cm^{-1} were attributed to C = O, amide bond, and C-O stretching vibrations, respectively [40].

It was found that the FTIR spectrum of HyA-DA-HPA showed peaks at 1750 cm^{-1} (C = O stretching) and 1200 cm^{-1} (C-N stretching) (figure 2). These results correspond to the expected structure of the chemical composition, suggesting that DA successfully conjugated to HyA via amide bond and the HyA-DA conjugated to HPA via amine groups of the HyA and succinimide ester active groups of the HPA. The chemical structure of HyA-DA conjugates with various concentrations of DA was characterized using ^1H NMR, as shown in figure S2. The N-acetyl peak of HyA backbone appeared at around 2 ppm. Multiples from 2.8 to 3.7 ppm are associated with the disaccharide unit and anomeric protons composed of d-glucuronic acid and N-acetyl-d-glucosamine in the HyA while the position between 6.7 and 7.2 ppm corresponds to the catechol ring of DA. Moreover, the area under this peak increased with an increasing DA feed ratio [25].

Figure 3(a) shows the ^1H NMR spectrum of HyA. The peak at δ 1.9 (number 1) ppm and the group peaks around δ 3.0–4.0 (number 2) ppm and δ 4.8 (number 3) ppm correspond to acetamidemethyl protons and protons from sugar ring and anomeric protons, respectively. The ^1H NMR spectrum of DA is shown in figure 3(b). The chemical shift assignments are based on the literature values [41, 42]. The lower-field portion of the spectrum (right) contains 2 triplets (number 1, 2) corresponding to the two methylene groups on the ethylamine portion of the molecule. The high field region (left) shows the aromatic protons (numbers 3, 4 and 5). The typical ^1H NMR spectra of HPA are shown in figure 3(c).

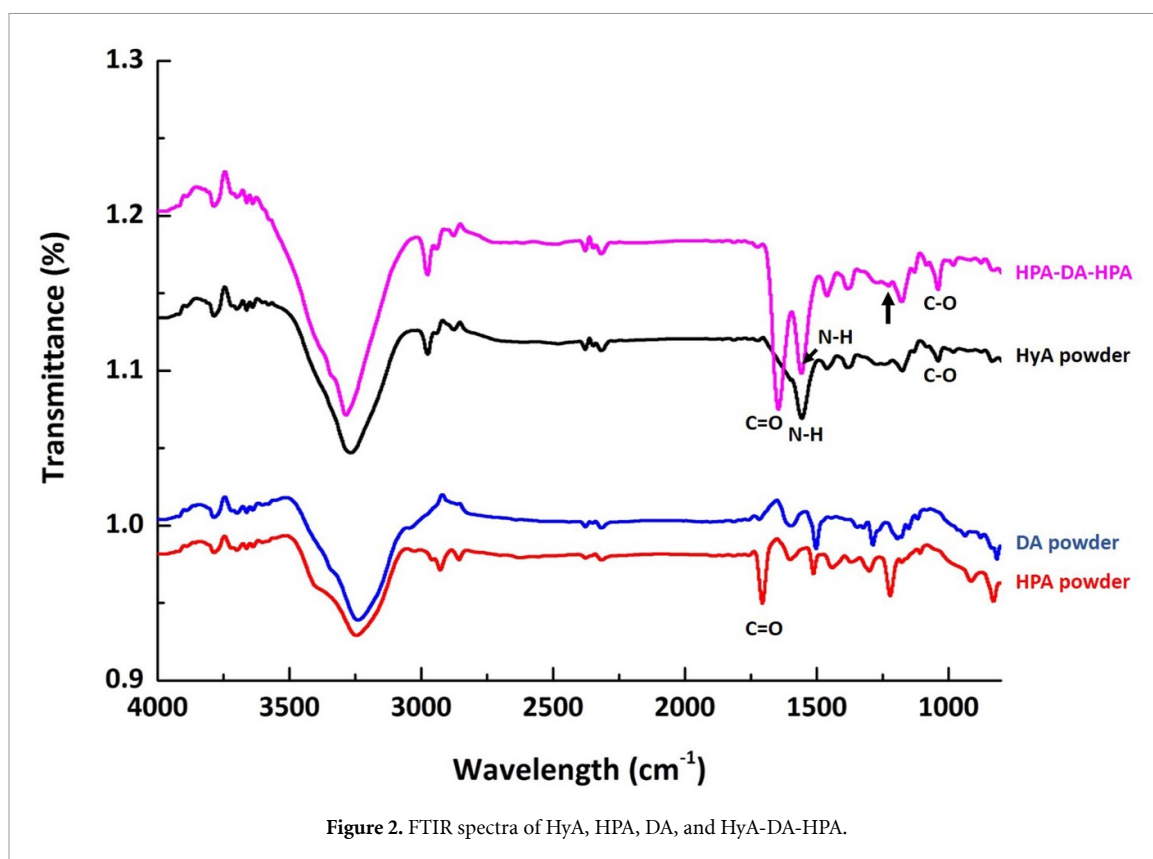


Figure 2. FTIR spectra of HyA, HPA, DA, and HyA-DA-HPA.

Figure 3(d) shows the ^1H NMR spectrum of HyA-DA with the appearance of the peaks at δ 6.95–6.60 ppm (number 6, 7, 8) corresponding to the H in the aromatic rings of grafted catechol moieties. The peaks at 2.8–3.0 ppm represent H in the methylene of DA chains. In figure 3(e), the spectrum of HyA-DA-HPA includes the spectra of HyA, DA, and HPA, confirming the successful grafting of HyA, DA, and HPA.

3.3. Morphology of HyA-DA-HPA

SEM images of a representative HyA-DA-HPA polymer and HyA-DA-HPA gel are shown in figures 4(a) and (b). A unique branched porous microstructure was found in the HyA-DA-HPA gel while the fibrous structure appeared in the HyA-DA-HPA polymer. Pores in the HyA-DA-HPA gel can serve as communication and transportation channels for cells and nutrients [6]. The estimated pore size based on the images ranges from 50 to 300 μm . HyA-DA-HPA hydrogel formation is shown in figure 4(c). The HyA-DA-HPA hydrogel formation occurred via the HRP-mediated coupling of the introduced phenol moieties. Coupling of phenols could take place either via a carbon-carbon bond at the ortho positions or via a carbon-oxygen bond between the carbon atom at the ortho and the phenoxy oxygen positions [43]. This is similar to the crosslinking of hyaluronic acid-tyramine (HyA-Tyr) conjugates via the oxidative coupling of Tyr moieties using HRP and H_2O_2 . HRP has been frequently used as a catalyst for the

oxidative coupling of phenol derivatives under mild reaction conditions [31]. In this case, the oxidative coupling of phenol proceeded at the C–C and C–O positions between phenols [44, 45].

3.4. Rheological measurement

The mechanical properties of the hydrogel were characterized at 37 $^\circ\text{C}$ using rheological measurement at various concentrations of HyA-DA-HPA: 0.5%, 1.0%, 1.5%, 1.75% and 2.0% (w/v) (figure 5). Higher concentrations of HyA-DA-HPA had higher storage moduli (G'), resulting in higher mechanical stability. Crosslinked HyA-DA-HPA gels exhibited storage moduli ranging from ~ 100 Pa to $\sim 20\,000$ Pa (at the frequency of 2000 rad s^{-1}) which are typical of a soft hydrogel and similar to native soft tissues [46]. Previously, with magnetic resonance elastography, the storage moduli (G') of the grey matter and white matter in the adult human brain are ~ 3.1 kPa and ~ 2.7 kPa, respectively [47]. Substrate elasticity also affects behaviors and fates of cells; for example, cell proliferation and differentiation of NSCs cultured in 3D alginate hydrogels varied with different elastic moduli, where the softest hydrogel with a modulus of ~ 180 Pa increased cell proliferation and resulted in the greatest enhancement in neuronal differentiation [48]. Adult NSCs also exhibited a higher neuronal differentiation on soft gels ($E = \sim 0.1$ – 0.5 kPa) and an enhanced glial differentiation on stiffer gels ($E = \sim 1$ – 10 kPa) [49]. Our results showed that as the concentration of the HyA-DA-HPA increased, the

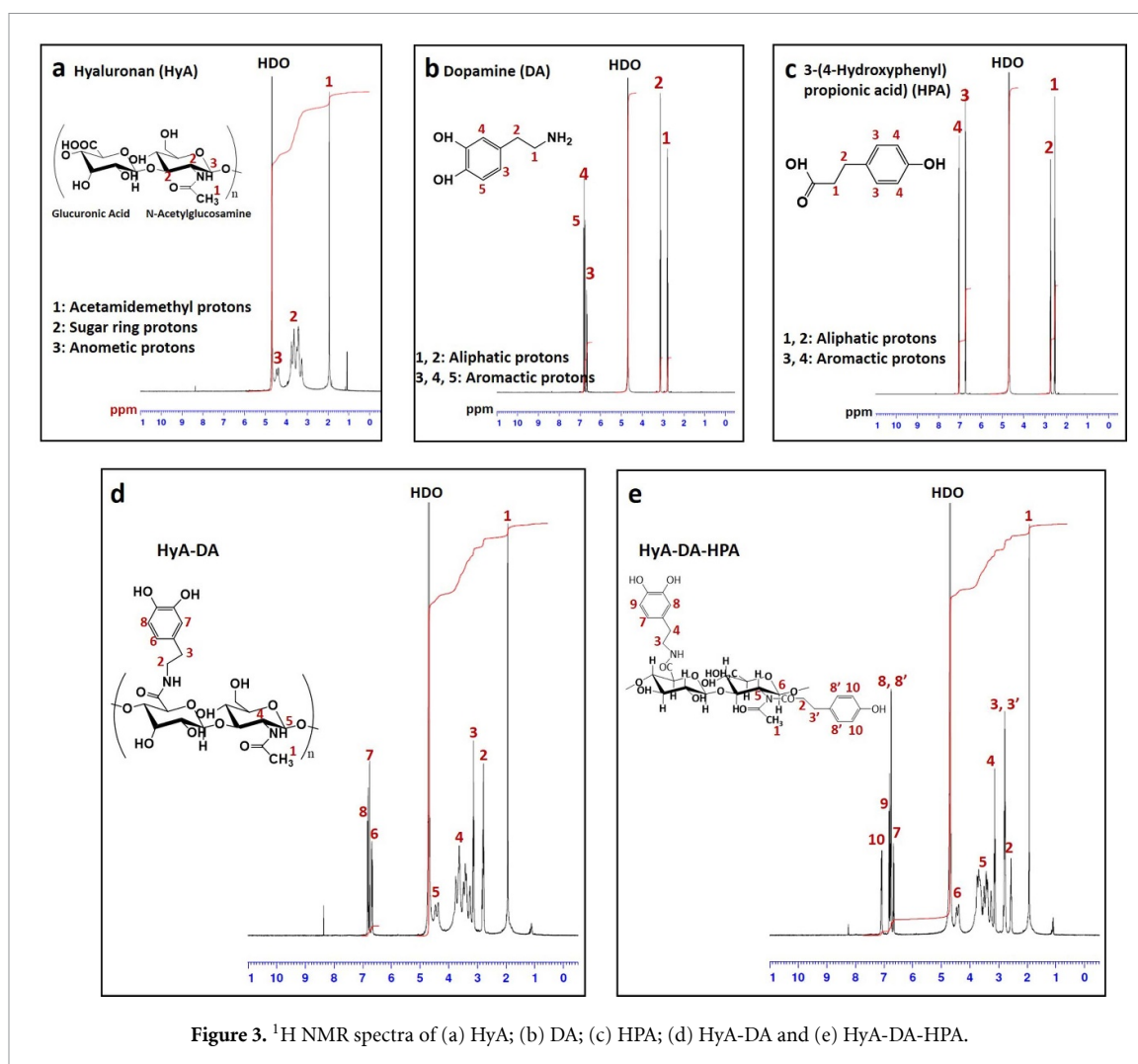


Figure 3. ¹H NMR spectra of (a) HyA; (b) DA; (c) HPA; (d) HyA-DA and (e) HyA-DA-HPA.

storage moduli increased due to the enhanced cross-linking. Hydrogels with storage moduli <500 Pa were excluded from the selection as these soft gels were too difficult to handle and they degraded within a few days even in *in vitro* cell cultures. Thus, HyA-DA-HPA with a concentration higher than 1.5 w/v% was preferred to use for *in vitro* studies.

3.5. Effect of HRP, H₂O₂, and polymer concentrations on gelation time

The gelation time was shown to be controllable by changing the concentration of HRP, H₂O₂, and polymer (figure 6). The gelation time decreased from 186 to 11 s as the HRP concentration increased from 0.05 to 0.24 U ml⁻¹ at a constant H₂O₂ concentration (1.0 μmol ml⁻¹) and polymer concentration (2.0 w/v%) (figure 6(a)). HRP allows the phenol substrate in the HyA-DA-HPA conjugate to couple each other via the carbon-carbon bond at the ortho position or via a carbon-oxygen bond between the carbon at the ortho position and the phenoxy oxygen in an aqueous solution [33, 50]. Thus, gelation time decreased as HRP concentration increased since the rate of creating phenoxy radicals increased in the coupling reaction. In contrast, as H₂O₂ concentration

increased from 0.15 to 1.0 μmol ml⁻¹, the gelation time slightly increased from 6.2 to 12.8 s (figure 6(b)). In the case of 0.15 μmol ml⁻¹ H₂O₂, a longer gelation time of the hydrogel occurred compared to 0.25 μmol ml⁻¹. This result was potentially due to the fact that a small number of phenoxy radicals were produced at a lower concentration of the catalyst, resulting in a delay of the crosslinking reaction. From 0.25 μmol ml⁻¹ H₂O₂ to 1.0 μmol ml⁻¹ H₂O₂, the gelation time increased due to the generation of an inactivated form of HRP caused by excessive H₂O₂. Faster gelation time was observed for higher polymer concentrations as shown in figure 6(c). This can be explained by a higher concentration of reactive phenol groups available with a higher polymer concentration and it increased the overall crosslinking reaction rate, facilitating gel formation.

3.6. Effect of H₂O₂ concentration on *in vitro* cell viability of MSCs

We selected MSCs as our cell model to test the biocompatibility of the hydrogels. The effect of H₂O₂ concentration on cell viability of MSCs was evaluated for finding the highest acceptable concentration of crosslinking reaction initiator. To achieve liable

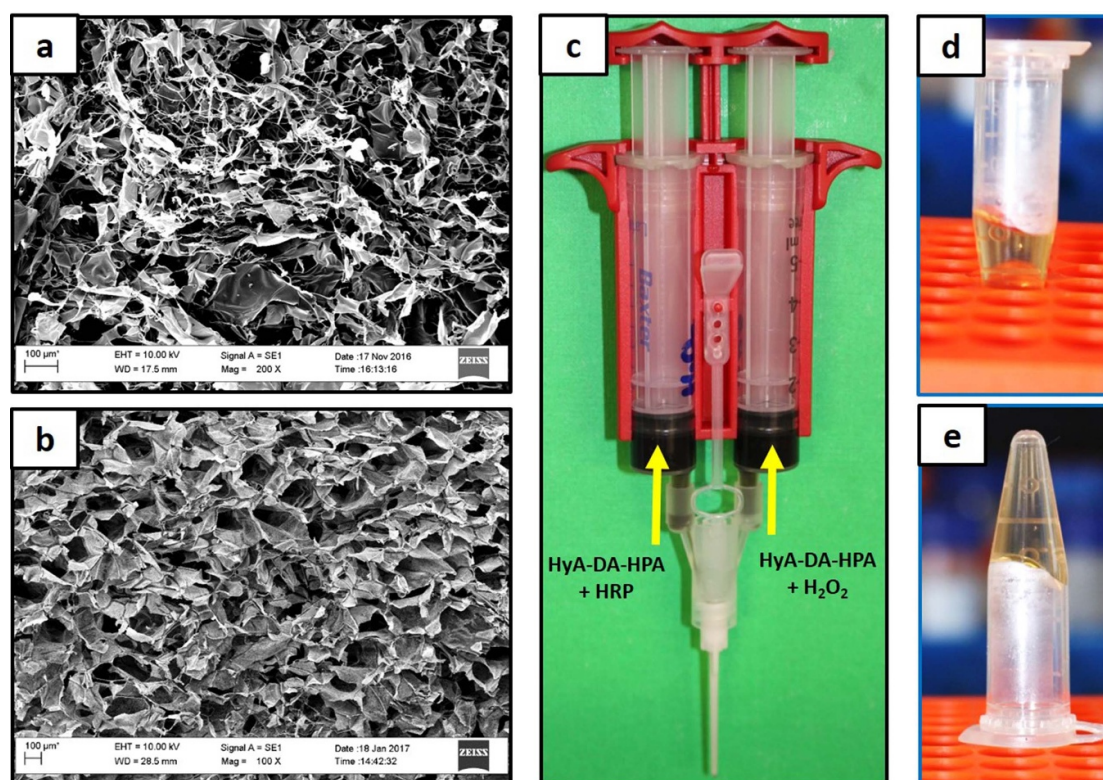


Figure 4. (a) Morphology of HyA-DA-HPA polymer before forming the gel; (b) with the addition of H₂O₂ and HRP, the gel was formed, then freeze dried and observed by SEM; (c) the HyA-DA-HPA hydrogel precursor was mixed with HRP and H₂O₂ using a double syringe system, which catalyzed gelation to form a hydrogel *in situ*; (d) and (e) the gel was formed after 10 s of mixing.

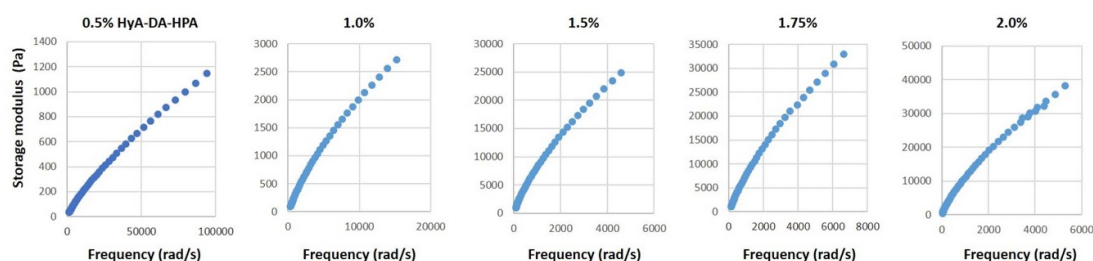


Figure 5. Rheological measurements of HyA-DA-HPA at various concentrations of polymers at the presence of HRP (0.24 U ml⁻¹) and H₂O₂ (1.0 μmol ml⁻¹).

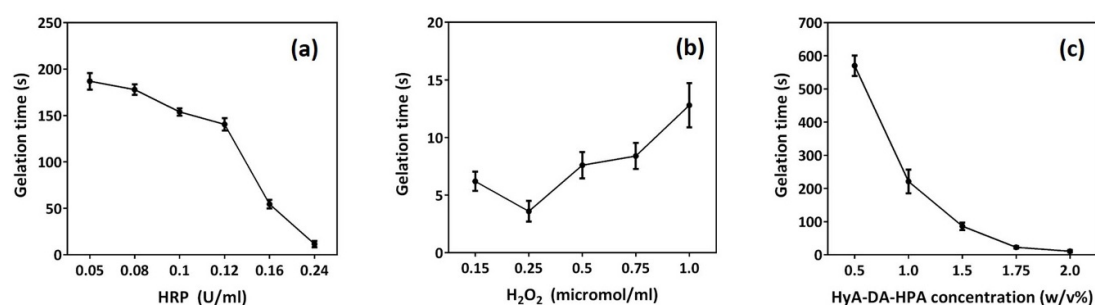
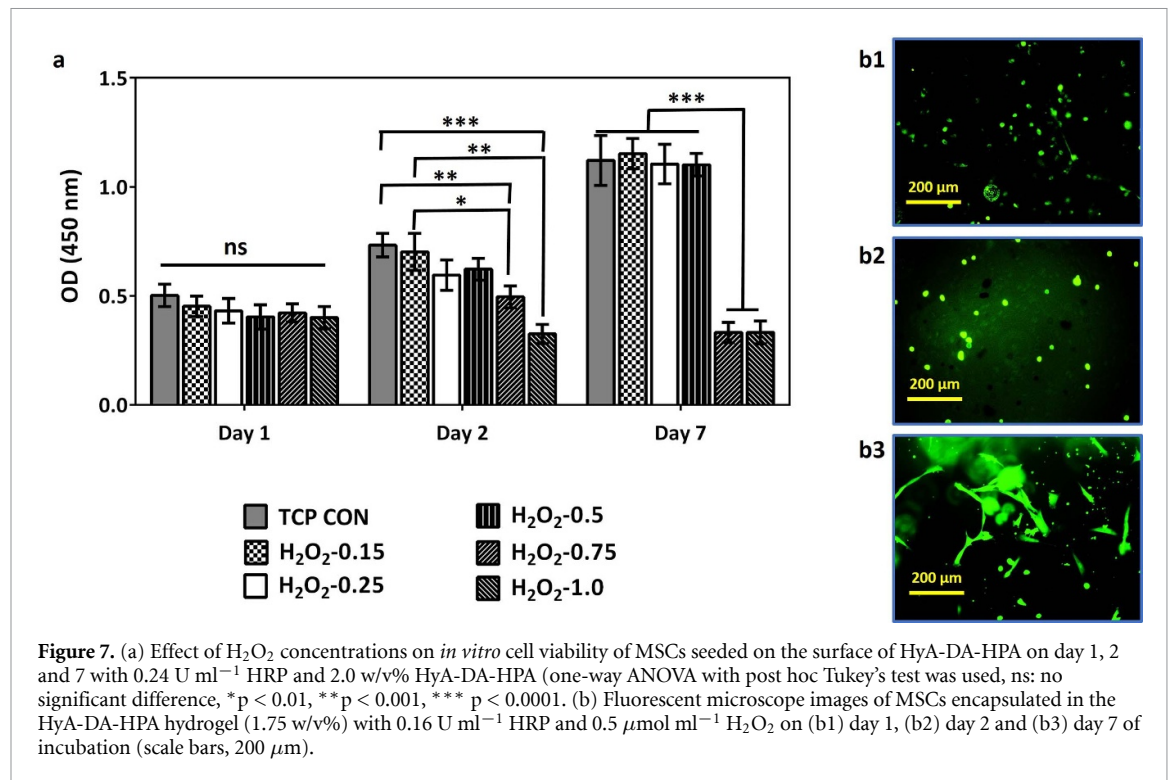


Figure 6. Gelation time of HyA-DA-HPA hydrogel at (a) different HRP concentrations (U ml⁻¹) with 1.0 μmol ml⁻¹ H₂O₂ and 2.0 w/v% HyA-DA-HPA; (b) different H₂O₂ concentrations (μmol ml⁻¹) with 0.24 U ml⁻¹ HRP and 2.0 w/v% HyA-DA-HPA and (c) different HyA-DA-HPA polymer concentrations (w/v%) with 0.24 U ml⁻¹ HRP and 1.0 μmol ml⁻¹ H₂O₂.



results from the CCK-8 cell viability assay, MSCs were cultured on top of the hydrogels for the cells to be fully immersed and in contact with the substrate of the CCK-8 assay. Different concentrations of H₂O₂ ranging from 0.15 to 1.0 μmol ml⁻¹ were tested as shown in figure 7(a). Cells cultured on top of the hydrogels retained their viability at 0.15, 0.25 and 0.5 μmol ml⁻¹ of H₂O₂. As a known cytotoxic agent, H₂O₂ at the higher concentrations of 0.75 and 1.0 μmol ml⁻¹ was toxic to the cells on day 2 and day 7. Thus, the concentration of H₂O₂ of 0.5 μmol ml⁻¹, the highest biocompatible concentration, was chosen as the most suitable parameter for the encapsulation of MSCs into the hydrogel. In terms of the cell morphology of the MSCs encapsulated in the HyA-DA-HPA hydrogels, cells exhibited mostly round morphology on day 1 and day 2 (figures 7(b1) and (b2)). However, on day 7 (figure 7(b3)), the cells performed spread morphology. It is possible that on day 1 and day 2, cells remained rounded within the hydrogel while they were embedded in a newly formed dense polymer network with low porosity. After days of culture, viable and functional MSCs degraded the matrix, attached and bound to the hydrogel scaffold, presenting a spread and elongated morphology. These results suggested that the cells could survive and that there was no cytotoxicity in the hydrogel matrix after 7 d. It also demonstrated our hydrogel platform as a promising material for MSC delivery since it can not only support the growth of cells encapsulated within but also display remodeling properties upon interaction with cells. This remodeling process can facilitate the integration of hydrogel with the ECM secreted by the encapsulated cells

and further bridge with the natural ECM in the transplanted sites, resulting in improved tissue adhesion and host integration [51].

3.7. Cellular responses of human iPSC-derived NSCs on HyA-DA-HPA hydrogels

Although MSCs have been shown to differentiate into neural lineages upon transplantation, their mechanisms could rely more on the trophic effects for neurogenesis, angiogenesis, and inflammatory and immune responses [52]. For example, transplantation of MSCs can increase expression levels of BDNF, insulin-like growth factor 1 (IGF-1), basic fibroblast growth factor (bFGF), vascular endothelial growth factor (VEGF), epidermal growth factor (EGF), and interleukin-10 (IL-10), etc, through direct secretion or activation of endogenous host cells to mediate cell apoptosis, survival, angiogenesis, and anti-inflammation to improve functional recovery [53–57]. Human iPSC-derived NSCs, which can bypass certain ethical issues compared to embryonic stem cell-derived progeny and can potentially lower the risk of immune rejection, have been reported as an alternative to treat brain injuries [58]. Compared to MSCs' trophic effects, these cells facilitate neuroregeneration and repair via neuronal protection, reducing microglia activation, and most importantly, long-term integration of differentiated neurons and glial cells [59–62]. We selected HyA-DA-HPA hydrogels (2.0 w/v%) made with 0.24 U ml⁻¹ HRP and 0.5 μmol ml⁻¹ H₂O₂ to assess its biocompatibility with human iPSC-derived NSCs, which express typical markers of NSCs (e.g. Pax6 and Nestin) and acquire the capability to differentiate

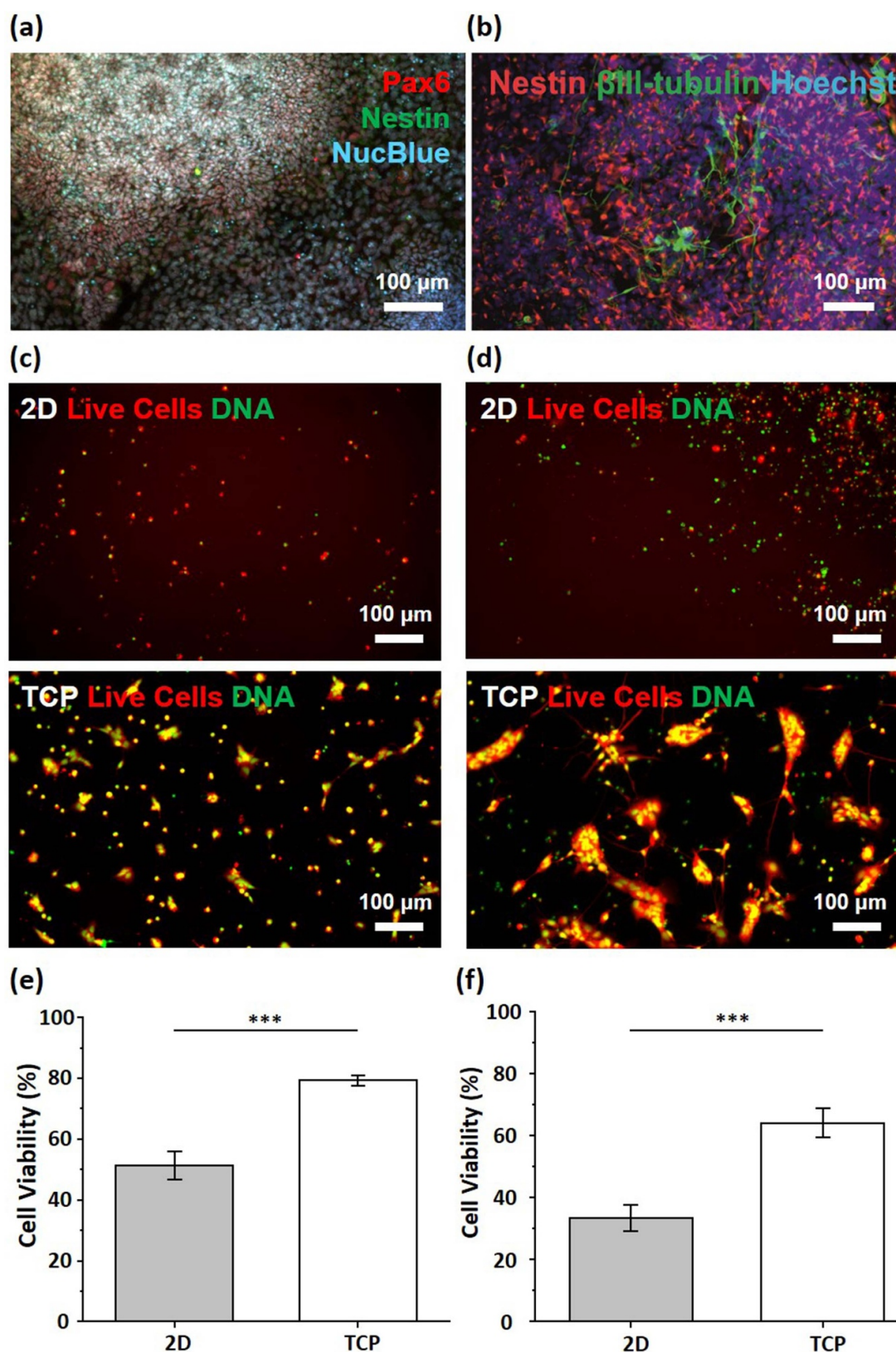


Figure 8. Cellular responses of human iPSC-derived NSCs on HyA-DA-HPA hydrogels synthesized with $0.5 \mu\text{mol ml}^{-1} \text{H}_2\text{O}_2$. (a), (b) Characterizations of human iPSC-derived NSCs, which express typical NSC markers, including Pax6 and Nestin, and can differentiate into $\beta\text{III-Tubulin}$ positive neurons. Cell viability assay was examined on (c), (e) day 1 and (d), (f) day 3 (scale bars, 100 μm). (Two-sample t-test was used. The results represent means \pm s.e.m. *** represents $p \leq 0.001$).

into $\beta\text{III-Tubulin}$ positive neurons (figures 8(a) and (b)). As the NSC culture media is serum free, we added $10 \mu\text{g ml}^{-1}$ laminin and 10 ng ml^{-1} BDNF

in the media to promote cell binding to the substrate and neuronal differentiation, respectively. On both day 1 and day 3, human iPSC-derived NSCs

on the hydrogels exhibited a round shape morphology while the cells on the TCP control were flattened and spread with typical neurite morphology (figures 8(c) and (d)). The cells cultured on the 2D hydrogel substrate exhibited significantly lower cell viability, $51.3 \pm 4.6\%$ and $33.3 \pm 3.7\%$ on day 1 and day 3, respectively, compared to the TCP control, which is $79.2 \pm 1.8\%$ and $64.0 \pm 4.3\%$ on day 1 and day 3, respectively (figures 8(e) and (f)). The discrepant cellular responses observed in the transformed MSC cell lines and human iPSC-derived NSCs might due to that iPSC-derived cultures are inherently more sensitive to their culture environment. Subtle effects of molecules released after gel degradation can affect the iPSC-derived NSCs while the MSCs remain unresponsive. We also observed that after incubation, the hydrogel acquired a large volume expansion, resulting in increased surface area. While in the MSC culture, the addition of 10% (v/v) FBS can sufficiently cover the internal structure of the expanded hydrogel, the provided laminin coating ($10 \mu\text{g ml}^{-1}$) in the iPSC-derived neural cultures, on the other hand, might no longer be able to supply adequate ECM protein after gel expansion and thus affect cell binding, attachment, viability, and growth. In the future, cell adhesion molecules can potentially be functionalized into our hydrogel polymer to improve cell attachment, proliferation, and growth. A higher concentration of BDNF can be incorporated into the hydrogel to support cell survival in the early phase of cell delivery.

DA as a neurotransmitter known to control movement and emotions has been used for local delivery to treat Parkinson's disease [63]. Application of hydrogel for delivery of DA or its agonists with or without incorporation of cells has been reported [24–26, 64, 65]. In general, the controlled release of molecules modulated via physical interactions (e.g. electrostatic interactions and hydrophobic association) possess a relatively short-term release compared to chemical conjugation methods, where the polymer immobilizes the drug and it is only released when the network degrades [66]. In our study, we chemically conjugated DA into our polymer backbones. Although we have not yet examined the release of DA from the hydrogel, the covalent linkages between DA and the backbone polymer might lead to a slower release compared to physical incorporation methods. As most neurological diseases require long-term therapy, this hydrogel might facilitate the treatment of these diseases. It has been shown that chemical modifications of a drug molecule might affect drug activity or property if it modifies molecules' active sites or causes a conformation change [67]. It is worth understanding whether our hydrogel could release functional DA molecules after degradation and if there are any side products formed after material degradation. Future works will focus on the characterization of the released products, their release

profile, and their effects on biocompatibility and cellular behaviors.

4. Conclusion

We have synthesized a novel hydrogel material based on HyA-DA-HPA. The gelation time of the HyA-DA-HPA hydrogel can be controlled from 3 s to 5 min by changing the concentration of HRP, H_2O_2 , and polymer. For specific applications, the hydrogel can be rapidly formed within 3 s under physiological conditions using HRP and H_2O_2 as catalysts for coupling. The effect of H_2O_2 concentration on cell viability was evaluated using MSCs. The synthesized hydrogel acquires no cytotoxicity, except for the hydrogels formed with 0.75 and $1.0 \mu\text{mol ml}^{-1}$ of H_2O_2 due to the cytotoxicity of the residual H_2O_2 . We also examined the biocompatibility of the hydrogel with human clinically relevant cell populations, human iPSC-derived NSCs. A decreased viability was observed and the results could be attributed to the release of the degradation products and the lack of cell binding sites. Initial *in vitro* studies revealed the potential of the encapsulation of MSCs inside the hydrogel. Future studies will include the detailed analysis of the effects of HRP, H_2O_2 , and polymer concentrations on the gel's stiffness and degradation time. Examination of the formation of any side products and their effects on biocompatibility, cell behaviors, and long term cell viability will be conducted to improve its biocompatibility with human clinically relevant cells.

Acknowledgments

This work was supported by funding provided by China Regenerative Medicine International (CRMI) and Jiangsu Industrial Technology Research Institute.

ORCID iDs

Linh T B Nguyen  <https://orcid.org/0000-0002-8532-8296>

Hua Ye  <https://orcid.org/0000-0001-7613-6041>

References

- [1] Richardson T P, Peters M C, Ennett A B and Mooney D J 2001 Polymeric system for dual growth factor delivery *Nat. Biotechnol.* **19** 1029–34
- [2] Sakai S, Hirose K, Taguchi K, Ogushi Y and Kawakami K 2009 An injectable, *in situ* enzymatically gellable, gelatin derivative for drug delivery and tissue engineering *Biomaterials* **30** 3371–7
- [3] Lee S H, Lee Y, Chun Y W, Crowder S W, Young P P, Park K D and Sung H-J 2014 *In situ* crosslinkable gelatin hydrogels for vasculogenic induction and delivery of mesenchymal stem cells *Adv. Funct. Mater.* **24** 6771–81
- [4] Jatav V S, Singh H and Singh S K 2011 Recent trends on hydrogel in human body *Int. J. Res. Pharm. Biomed. Sci.* **2** 442–7

- [5] George J, Hsu -C-C, Nguyen L T B, Ye H and Cui Z 2019 Neural tissue engineering with structured hydrogels in CNS models and therapies *Biotechnol. Adv.* accepted (<https://doi.org/10.1016/j.biotechadv.2019.03.009>)
- [6] Riley C M, Fuegy P W, Firpo M A, Zheng Shu X, Prestwich G D and Peattie R A 2006 Stimulation of in vivo angiogenesis using dual growth factor-loaded crosslinked glycosaminoglycan hydrogels *Biomaterials* **27** 5935–43
- [7] Nih L R, Carmichael S T and Segura T 2016 Hydrogels for brain repair after stroke: an emerging treatment option *Curr. Opin. Biotechnol.* **40** 155–63
- [8] McCrory B, LaGrange C A and Hallbeck M 2014 Quality and safety of minimally invasive surgery: past, present, and future *Biomed. Eng. Comput. Biol.* **6** 1–11
- [9] Chan H H, Wathen C A, Ni M and Zhuo S 2017 Stem cell therapies for ischemic stroke: current animal models, clinical trials and biomaterials *RSC Adv.* **7** 18668–80
- [10] Tuladhar A, Payne S L and Shoichet M S 2018 Harnessing the potential of biomaterials for brain repair after stroke *Front. Mater.* **5** 14
- [11] Ford M C, Bertram J P, Hynes S R, Michaud M, Li Q, Young M, Segal S S, Madri J A and Lavik E B 2006 A macroporous hydrogel for the coculture of neural progenitor and endothelial cells to form functional vascular networks *in vivo* *Proc. Natl. Acad. Sci. USA* **103** 2512–17
- [12] Marchini A, Raspa A, Pugliese R, El Malek M A, Pastori V, Lecchi M, Vescovi A L and Gelain F 2019 Multifunctionalized hydrogels foster hNSC maturation in 3D cultures and neural regeneration in spinal cord injuries *Proc. Natl. Acad. Sci. USA* **116** 7483–92
- [13] Barros C S, Franco S J and Müller U 2011 Extracellular matrix: functions in the nervous system *Cold Spring Harbor Perspect. Biol.* **3** a005108
- [14] Broguiere N, Isenmann L and Zenobi-Wong M 2016 Novel enzymatically cross-linked hyaluronan hydrogels support the formation of 3D neuronal networks *Biomaterials* **99** 47–55
- [15] Liu L, Liu Y, Li J, Du G and Chen J 2011 Microbial production of hyaluronic acid: current state, challenges, and perspectives *Microb. Cell Fact.* **10** 99
- [16] Lin C-M *et al* 2009 Hyaluronic acid inhibits the glial scar formation after brain damage with tissue loss in rats *Surg. Neurol.* **72** S50–4
- [17] Aurand E R, Lampe K J and Bjugstad K B 2012 Defining and designing polymers and hydrogels for neural tissue engineering *Neurosci. Res.* **72** 199–213
- [18] Li Y, Rodrigues J and Tomas H 2012 Injectable and biodegradable hydrogels: gelation, biodegradation and biomedical applications *Chem. Soc. Rev.* **41** 2193–221
- [19] Liang Y, Walczak P and Bulte J W M 2013 The survival of engrafted neural stem cells within hyaluronic acid hydrogels *Biomaterials* **34** 5521–9
- [20] Moshayedi P, Nih L R, Llorente I L, Berg A R, Cinkornpumin J, Lowry W E, Segura T and Carmichael S T 2016 Systematic optimization of an engineered hydrogel allows for selective control of human neural stem cell survival and differentiation after transplantation in the stroke brain *Biomaterials* **105** 145–55
- [21] Adil M M, Vazin T, Ananthanarayanan B, Rodrigues G M C, Rao A T, Kulkarni R U, Miller E W, Kumar S and Schaffer D V 2017 Engineered hydrogels increase the post-transplantation survival of encapsulated hESC-derived midbrain dopaminergic neurons *Biomaterials* **136** 1–11
- [22] Nekrasov P V and Vorobyov V V 2018 Dopaminergic mediation in the brain aging and neurodegenerative diseases: a role of senescent cells *Neural Regen. Res.* **13** 649–50
- [23] Jia Z, Zhu H, Misra B R, Li Y and Misra H P 2008 Dopamine as a potent inducer of cellular glutathione and NAD(P)H: quinone oxidoreductase 1 in PC₁₂ neuronal cells: a potential adaptive mechanism for dopaminergic neuroprotection *Neurochem. Res.* **33** 2197–205
- [24] Kang K S, Lee S-I, Hong J M, Lee J W, Cho H Y, Son J H, Paek S H and Cho D-W 2014 Hybrid scaffold composed of hydrogel/3D-framework and its application as a dopamine delivery system *J. Control. Release* **175** 10–16
- [25] Ren Y, Zhao X, Liang X, Ma P X and Guo B 2017 Injectable hydrogel based on quaternized chitosan, gelatin and dopamine as localized drug delivery system to treat Parkinson's disease *Int. J. Biol. Macromol.* **105** 1079–87
- [26] Senthilkumar K S, Saravanan K, Chandra G, Sindhu K, Jayakrishnan A and Mohanakumar K 2007 Unilateral implantation of dopamine-loaded biodegradable hydrogel in the striatum attenuates motor abnormalities in the 6-hydroxydopamine model of hemi-parkinsonism *Behav. Brain Res.* **184** 11–18
- [27] Shin M, Kim H K and Lee H 2014 Dopamine-loaded poly(D,L-lactic-co-glycolic acid) microspheres: new strategy for encapsulating small hydrophilic drugs with high efficiency *Biotechnol. Prog.* **30** 215–23
- [28] Miao T, Wang J, Zeng Y, Liu G and Chen X 2018 Polysaccharide-based controlled release systems for therapeutics delivery and tissue engineering: from bench to bedside *Adv. Sci.* **5** 1700513
- [29] Lee Y, Bae J W, Oh D H, Park K M, Chun Y W, Sung H-J and Park K D 2013 *In situ* forming gelatin-based tissue adhesives and their phenolic content-driven properties *J. Mater. Chem. B* **1** 2407–14
- [30] Moreira Teixeira L S, Bijl S, Pully V V, Otto C, Jin R, Feijen J, van Blitterswijk C A, Dijkstra P J and Karperien M 2012 Self-attaching and cell-attracting in-situ forming dextran-tyramine conjugates hydrogels for arthroscopic cartilage repair *Biomaterials* **33** 3164–74
- [31] Teixeira L S M, Feijen J, van Blitterswijk C A, Dijkstra P J and Karperien M 2012 Enzyme-catalyzed crosslinkable hydrogels: emerging strategies for tissue engineering *Biomaterials* **33** 1281–90
- [32] Saptari V 2003 *Fourier-Transform Spectroscopy Instrumentation Engineering* (Bellingham, WA: SPIE Press)
- [33] Jin R, Hiemstra C, Zhong Z and Feijen J 2007 Enzyme-mediated fast in situ formation of hydrogels from dextran-tyramine conjugates *Biomaterials* **28** 2791–800
- [34] Kurisawa M, Chung J E, Yang Y Y, Gao S J and Uyama H 2005 Injectable biodegradable hydrogels composed of hyaluronic acid-tyramine conjugates for drug delivery and tissue engineering *Chem. Commun.* **34** 4312–14
- [35] Linh N T B, Abueva C D and Lee B-T 2017 Enzymatic *in situ* formed hydrogel from gelatin-tyramine and chitosan-4-hydroxyphenyl acetamide for the co-delivery of human adipose-derived stem cells and platelet-derived growth factor towards vascularization *Biomed. Mater.* **12** 015026
- [36] Mihara K, Imai C, Coustan-Smith E, Dome J S, Dominici M, Vanin E and Campana D 2003 Development and functional characterization of human bone marrow mesenchymal cells immortalized by enforced expression of telomerase *Br. J. Haematol.* **120** 846–9
- [37] Bilican B *et al* 2012 Mutant induced pluripotent stem cell lines recapitulate aspects of TDP-43 proteinopathies and reveal cell-specific vulnerability *Proc. Natl. Acad. Sci. USA* **109** 5803–8
- [38] Hsu -C-C, Serio A, Amdursky N, Besnard C and Stevens M M 2018 Fabrication of hemin-doped serum albumin-based fibrous scaffolds for neural tissue engineering applications *ACS Appl. Mater. Interfaces* **10** 5305–17
- [39] Chambers S M, Fasano C A, Papapetrou E P, Tomishima M, Sadelain M and Studer L 2009 Highly efficient neural conversion of human ES and iPS cells by dual inhibition of SMAD signaling *Nat. Biotechnol.* **27** 275–80
- [40] Lih E, Choi S G, Ahn D J, Joung Y K and Han D K 2016 Optimal conjugation of catechol group onto hyaluronic acid in coronary stent substrate coating for the prevention of restenosis *J. Tissue Eng.* **7** 1–11
- [41] Demura M, Yoshida T, Hirokawa T, Kumaki Y, Aizawa T, Nitta K, Bitter I and Tóth K 2005 Interaction of dopamine and acetylcholine with an amphiphilic resorcinarene

- receptor in aqueous micelle system *Bioorg. Med. Chem. Lett.* **15** 1367–70
- [42] Bisaglia M, Mammi S and Bubacco L 2007 Kinetic and structural analysis of the early oxidation products of dopamine analysis of the interactions with α -synuclein *J. Biol. Chem.* **282** 15597–605
- [43] Phuong N T, Anh Ho V, Hai Nguyen D, Khoa N C, Quyen T N, Lee Y and Park K D 2015 Enzyme-mediated fabrication of an oxidized chitosan hydrogel as a tissue sealant *J. Bioact. Compat. Polym.* **30** 412–23
- [44] Wang L-S, Lee F, Lim J, Du C, Wan A C A, Lee S S and Kurisawa M 2014 Enzymatic conjugation of a bioactive peptide into an injectable hyaluronic acid–tyramine hydrogel system to promote the formation of functional vasculature *Acta. Biomater.* **10** 2539–50
- [45] Lee F, Chung J E and Kurisawa M 2009 An injectable hyaluronic acid–tyramine hydrogel system for protein delivery *J. Control. Release* **134** 186–93
- [46] Hinz B 2007 Formation and function of the myofibroblast during tissue repair *J. Invest. Dermatol.* **127** 526–37
- [47] Green M A, Bilston L E and Sinkus R 2008 *In vivo* brain viscoelastic properties measured by magnetic resonance elastography *NMR Biomed.* **21** 755–64
- [48] Banerjee A, Arha M, Choudhary S, Ashton R S, Bhatia S R, Schaffer D V and Kane R S 2009 The influence of hydrogel modulus on the proliferation and differentiation of encapsulated neural stem cells *Biomaterials* **30** 4695–9
- [49] Saha K, Keung A J, Irwin E F, Li Y, Little L, Schaffer D V and Healy K E 2008 Substrate modulus directs neural stem cell behavior *Biophys. J.* **95** 4426–38
- [50] Veitch N C 2004 Horseradish peroxidase: a modern view of a classic enzyme *Phytochemistry* **65** 249–59
- [51] Moroni L and Elisseeff J H 2008 Biomaterials engineered for integration *Mater. Today* **11** 44–51
- [52] Toyoshima A, Yasuhara T and Date I 2017 Mesenchymal stem cell therapy for ischemic stroke *Acta. Med. Okayama* **71** 263–8
- [53] Zhang J, Li Y, Chen J, Yang M, Katakowski M, Lu M and Chopp M 2004 Expression of insulin-like growth factor 1 and receptor in ischemic rats treated with human marrow stromal cells *Brain Res.* **1030** 19–27
- [54] Wakabayashi K *et al* 2010 Transplantation of human mesenchymal stem cells promotes functional improvement and increased expression of neurotrophic factors in a rat focal cerebral ischemia model *J. Neurosci. Res.* **88** 1017–25
- [55] Li J *et al* 2010 Human mesenchymal stem cell transplantation protects against cerebral ischemic injury and upregulates interleukin-10 expression in *Macaca fascicularis* *Brain Res.* **1334** 65–72
- [56] Chen J, Li Y, Katakowski M, Chen X, Wang L, Lu D, Lu M, Gautam S C and Chopp M 2003 Intravenous bone marrow stromal cell therapy reduces apoptosis and promotes endogenous cell proliferation after stroke in female rat *J. Neurosci. Res.* **73** 778–86
- [57] Kurozumi K *et al* 2004 BDNF gene-modified mesenchymal stem cells promote functional recovery and reduce infarct size in the rat middle cerebral artery occlusion model *Mol. Ther.* **9** 189–97
- [58] Willerth S M 2011 Neural tissue engineering using embryonic and induced pluripotent stem cells *Stem Cell Res. Ther.* **2** 17
- [59] Baker E W *et al* 2017 Induced pluripotent stem cell-derived neural stem cell therapy enhances recovery in an ischemic stroke pig model *Sci. Rep.* **7** 10075
- [60] Laterza C, Uoshima N, Tornero D, Wilhelmsson U, Stokowska A, Ge R, Pekny M, Lindvall O and Kokaia Z 2018 Attenuation of reactive gliosis in stroke-injured mouse brain does not affect neurogenesis from grafted human iPSC-derived neural progenitors *PLoS One* **13** e0192118
- [61] Tornero D *et al* 2013 Human induced pluripotent stem cell-derived cortical neurons integrate in stroke-injured cortex and improve functional recovery *Brain* **136** 3561–77
- [62] Wernig M, Zhao J-P, Pruszak J, Hedlund E, Fu D, Soldner F, Broccoli V, Constantine-Paton M, Isacson O and Jaenisch R 2008 Neurons derived from reprogrammed fibroblasts functionally integrate into the fetal brain and improve symptoms of rats with Parkinson's disease *Proc. Natl. Acad. Sci. USA.* **105** 5856–61
- [63] Jaber M, Robinson S W, Missale C and Caron M G 1996 Dopamine receptors and brain function *Neuropharmacology* **35** 1503–19
- [64] Komatsu M, Konagaya S, Egawa E Y and Iwata H 2015 Maturation of human iPS cell-derived dopamine neuron precursors in alginate–Ca²⁺ hydrogel *Biochim. Biophys. Acta. Gen. Subj.* **1850** 1669–75
- [65] Proctor C M, Chan C Y, Porcarelli L, Udabe E, Sanchez-Sanchez A, Del Agua I, Mecerreyes D and Malliaras G G 2019 An ionic hydrogel for accelerated dopamine delivery via retrodialysis *Chem. Mater.* **31** 7080–4
- [66] Li J and Mooney D J 2016 Designing hydrogels for controlled drug delivery *Nat. Rev. Mater.* **1** 16071
- [67] Alconcel S N S, Baas A S and Maynard H D 2011 FDA-approved poly(ethylene glycol)–protein conjugate drugs *Polym. Chem.* **2** 1442–8